https://doi.org/10.22645/udi.2018.7.1.005
도시과학 제7권 제1호 2018. 6 5-9쪽

Cyclic behavior of superelastic shape memory alloys (SMAs) under various loading conditions

Jong Wan Hu*

Abstract: The nickel-titanium shape memory alloy (SMA), referred to as Nitinol, exhibits a superelastic effect that can be restored to its original shape even if a significant amount of deformation is applied at room temperature, without any additional heat treatment after removal of the load. Owing to these unique material characteristics, it has widely used as displacement control devices for seismic retrofitting in civil engineering fields as well as medical, electrical, electronic and mechanical fields. Contrary to ordinarty carbon steel, superelastic SMAs are very resistant to fatigue, and have force-displacement properties depending on loading speed. The change for the mechanical properties of superelastic SMAs are experimentally inviestigated in this study when loading cycle numbers and loading speeds are different. In addition, the standardized force-displacement properties of such superelastic SMAs are proposed with an aim to efficiently design the seismic retrofitting devices made of these materials.

Key Words: Superelastic effect, Shape memory alloy (SMA), Fatigue cyclic loading, Loading Speed, Residual deformation

1. Introduction

Unlike ordinary carbon steel where residual deformation occurs after imposing the elastic limit, the superelastic shape memory alloy (SMA) retains the configuration memorized at the time of material creation. Even if a substantial amount of deformation takes place due to an external impact, this special metal can restore original shape only after the removal of stress at room temperature [1]. Because of the unique material properties of these superelastic SMAs, life products such as metal stents, antennas, spectacle frames, braziers, and actuators have been widely used as the smart devices. Recently, manufacturing costs have been lowered owing to the development of material technology, and thus it has started to be used in construction fields such as connection bolts, earthquake rehabilitation devices, seismic restrainers, damper systems. Furthermore, related studies are being carried out at the laboratory stage [2-3].

The superelastic SMA materials have outstanding mechanical strength and fatigue resistance, and reduce residual strain with recentering force as compared with other metallic materials [1]. Contrary to ordinary carbon steel, strength, and residual strain characteristics presented in the stress-strain curves of such superelastic SMA materials vary in accordance with loading speed. In order to design accurate and efficient seismic retrofitting devices (i.e., dampers and isolators) made of superelastic SMAs, it is necessary to grasp the mechanical characteristics of these materials according to various loading speeds as well as different fatigue cycles. Most of the superelastic SMA devices are designed by utilizing material properties obtained by the static loading test without considering fatigue and loading speed. For this reason, there is a limit to some extend of accurately estimating the performance of the device under different seismic loads with different durations and speeds. Therefore, this study is intended to investigate the mechanical properties of superelastic SMA specimens by varying the number of loading cycles and loading speeds. Thereafter, we can also observe the post-yield strength and residual strain of these specimens in the obtained force-displacement curve.

* Professor, Department of Civil and Environmental Engineering, Incheon National university, Incheon 22012, Republic of Korea, Corresponding author(jongp24@inu.ac.kr)

2. Test Set-up

Figure 1 shows a specimen installed in a UTM device and the size of superelastic SMA specimens prepared in accordance with ASTM regulations for material testing [4]. In this study, dynamic loading tests were carried out under the displacement-controlled loading history under different loading speeds, and quasi-static fatigue tests were conducted as well with different loading cycles under the same loading speed. Each of specimens uniformly has 3mm thickness while the effective width and length were designed to be 25mm and 60mm, respectively. The average stress-strain curves of the material specimens used in the experimental tests are presented in Figure 2. The loading history was imposed on the specimens with the target strain of 1%, 3%, and 5% by the displacement control method. Finally, ultimate strain was applied until failure occurred. The loading speed was also 0.033mm/sec for three specimens measuring the stress-strain property curves.

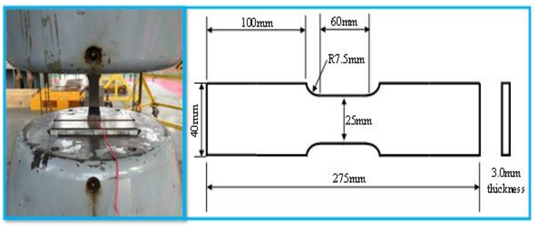

Figure 1. Overview of the experimental test set-up and specimen size.

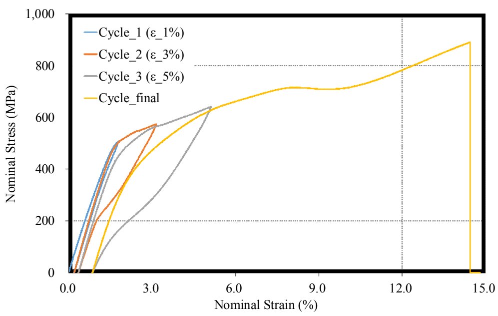

Figure 2. Material property of the superelastic SMA specimens.

The superelastic SMAs used in this study are a nitinol alloy made by mixing nickel and titanium at almost the same atomic ratio. They are composed of 55% of nickel and 45% of titanium. The temperature at which austenitic phase transformation starts is in the range of minus 15° C to minus 10° C . The material tests were carried out at room temperature of 25° C in order to obtain the stress-strain curves. These curves exhibit an initial elastic slope of about 30GPa, and martensitic phase transformation starts to occur at yield stress of 510MPa, corresponding to about 1.8% strain. The strain of 2-3% is almost recovered to orgianl configuration after the removal of the applied load. However, as strain imposed on the specimens gradually increases, residual strain also starts to increase. The stress of about 620MPa is generated at 5% strain, and then necking phenomeon occurrs at approximately 9% strain. Stress hardening take places after that, and finally the specimen is broken near 14.8% strain rate.

3. Loading Conditions

Figures 3 and 4 show the hysteresis curves of the quasi-static cyclic loading history used for the fatigue test and those of the dynamic loading history with different loading speed, respectively. As shown in Figure 3, N1, N10, and N25 of the model ID indicates the number of repeatedly applied times at the target strain of 5% corresponding to 3mm displacement. The same loading speed of 0.303mm/sec corresponding to 0.05Hz was applied for the fatigue test with quasi-static cyclic loading. After 5% target strain, 7% strain was applied, and final strain was imposed on the specimen until ultimate fracture decisively occurred. In case of dynamic loads, experimental tests were performed by applying a triangular sawtooth displacement-controlled load history, which gradually increases the amplitude of the displacement load cycle (Δ_{cycle}), to the material specimen. Basically, the same displacement-controlled load hysteresis curves were used for five models, but material experiments were performed with different loading speeds (i.e., 0.033mm/sec for SMA-1, 0.165mm/sec for SMA-2, 0.330mm/sec for SMA-3, 1.650mm/sec for SMA-4, and 3.300mm/sec for SMA-5model).

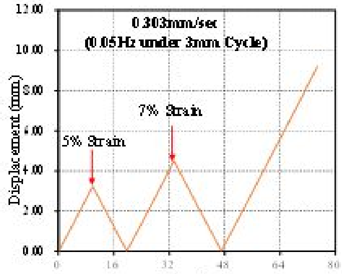

(a) SMA-N1

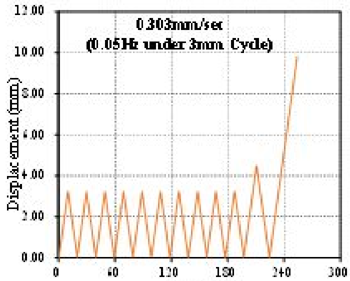

(b) SMA-N10

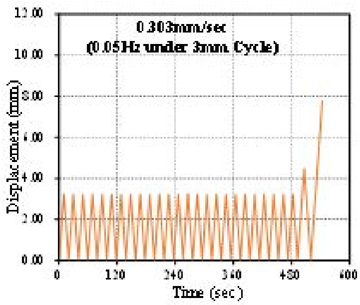

(c) SMA-N25

Figure 3. Loading protocols for quasi-static cyclic tests.

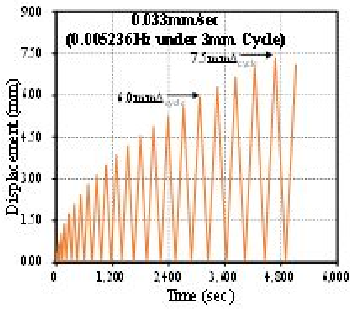

(a) SMA-1

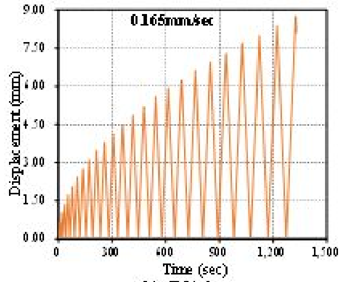

(b) SMA-2

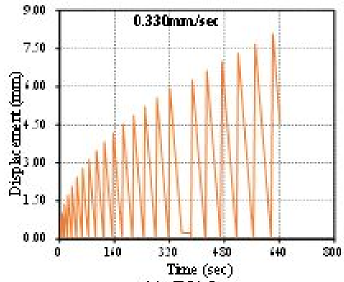

(c) SMA-3

Figure 4. Loading protocols for dynamic tests.

4. Test Results

Figure 5 shows force-displacement hysteresis curves obtained by applying the displacement-controlled load histories presented in Figures 3 and 4 to the material specimens. As can be seen in Figure 5(a), the fatigue test results shows almost the same strength performance in the hysteresis curves after the yield point at which the martensitic phase displacement occurs in three material specimens. This means that the superelastic SMA can reproduce the nearly same force-displacement behavior irrespective of the number of loading cycles, and does not change the mechanical properties by fatigue.

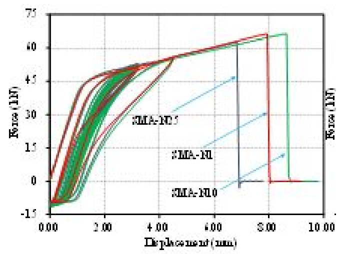

(a) Qunsi-static Cyclic Test

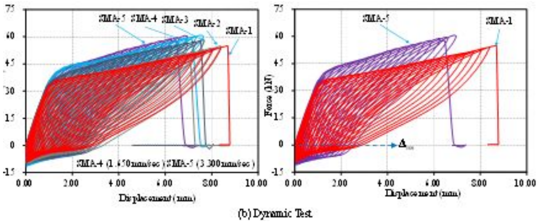

Figure 5. Experimental test results.

Figure 5 (b) shows the force-displacement curves obtained from dynamic tests with different loading speeds. In case of the SMA-1 model with the slowest loading speed, the maximum displacement exceeded 8.25mm, and thus the best displacement performance among five material specimens is shown. However, after the yield point where martensitic phase displacement begins to occur, strength performance is the lowest among five material specimens. On the other hand, the SMA-5 model with the fastest loading speed can be found in the hysteresis curve to allow the smallest maximum displacement in spite of showing the greatest strength performance after the yield point. At a displacement of about 7mm, the SMA-5 model has a load of 60kN, while the SMA-1 model shows a load performance of about 47kN. Therefore, as loading speed increases, strength performance improves, but maximum displacement allowed before the fracture occurs is reduced. The performance of typical seismic retrofitting systems is designed by applying the mechanical material properties obtained in a quasi-static load state with a low loading speed. Therefore, it can be assumed that the superelastic SMA devices under a seismic load having a relatively fast loading speed exhibit greater resistance than strength performance applied at static loading design.

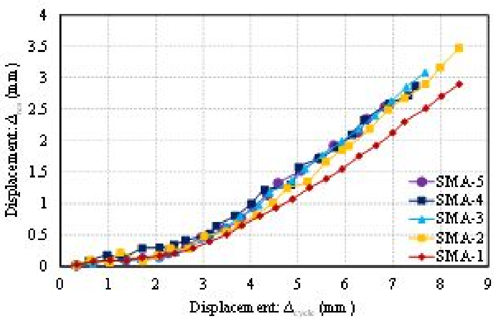

Figure 6. Comparison for residual displacements along measurement displacement load cycles.

For the purpose of understanding the recentering capacity of the superelastic SMA material specimens according to the loading speed, residual displacement (Δ_{res}) was measured at the point (refer to Figure 5(b)) where force was zero in the path after removing the applied load in each displacement load cycle (Δ_{cycle}). Figure 6 presents the plotted curves of the residual displacements measured along the corresponding path of displacement load cycles. In the same displacement load cycle, the SMA-1 model has the least residual displacement. The remaining four material specimens display almost similar residual displacement distributions, but the SMA-2 model, which has a relatively slower loading speed, exhibits smaller displacement distribution. It can be seen that as the loading speed increases, the amount of residual strain is increased by reducing recentering force generated in the material specimen. For example, the SMA-1 model shows 1mm residual displacement under 5mm displacement load cycle, while the SMA-5 model shows a 1.5mm residual displacement. Therefore, in this study, it can be concluded that the mechanical properties of the superelastic SMA materials utilized for seismic retrofitting design, change when the loading speed is varied.

5. Conclusion

In this study, we investigated superelastic shape memory alloy which can be used as a damper in a construction site. The experimental results of the superelastic shape memory alloy, which is the subject of the study, reduce the occurrence of residual displacement based on excellent restoring force. The superelastic shape memory alloy exhibits flagship hysteretic behavior with improved energy dissipation capability when quasi-static cyclic loading is applied by controlling displacement at room temperature. Based on the results of this study, it can be concluded that the superelastic shape memory alloy can be effectively used for earthquake load under high speed load condition instead of low speed static load. In the future, it will be possible to develop a seismic design method with improved performance if a super - elastic shape memory alloy is applied to seismic system.

Acknowledgments

This research was supported by a grant (18TBIP-C144315-01) from Technology Business Innovation Program (TBIP) Program funded by Ministry of Land, Infrastructure and Transport of Korean government.

REFERENCES

Song, G., Ma, N. and Li, .H. N. (2006) "Applications of shape memory alloys in civil structures", Eng. Struct. Vol. 28, pp. 1266.

Seo, J. and Hu, J. W. (2016) "Seismic Response and Performance Evaluation of Self-Centering LRB Isolators Installed on the CBF Building under NF Ground Motions", Sustainability, Vol. 8, pp. 109.

Hu, J. W. and Leon, R. T. (2011) "Analyses and evaluations for composite-moment frames with SMA PR-CFT connections", Nonlin. Dyna. Vol. 65, pp. 433.

ASTM Standard ASTM A370-17 (2006) Standard Test Method and Definition for Mechanical Testing of Steel Product, West Conshohocken, PA, USA.

논문투고일: 6월 19일
논문게재일: 6월 30일